- Technical Paper -

INVESTIGATION ON THE SHEAR OF FIBER REINFORCED CONCRETE BEAMS CONSIDERING VARIOUS TYPES OF FIBERS

Pitcha JONGVIVATSAKUL*1, Koji MATSUMOTO*2, Ken WATANABE*3 and Junichiro NIWA*4

ABSTRACT

This paper presents the evaluation of shear carried by fibers in fiber reinforced concrete beams (FRC) using tension softening curves. Four FRC beams with various kinds of fibers, which were made by steel with length of 30 mm and 60 mm, polypropylene with 30 mm length, and polyvinyl alcohol with 30 mm length, were tested. The tension softening curve was used for calculating the force transferred across the diagonal crack from its width, which was measured through the image analyzing system. The calculated shear carried by fibers showed good correspondence with the experimental results.
Keywords: shear carried by fibers, steel fibers, polypropylene fibers, polyvinyl alcohol fibers, tension softening curves

1. INTRODUCTION

Shear failure of reinforced concrete (RC) beams is known to be brittle and catastrophic. After the occurrence of diagonal crack, the tensile stress at the crack surfaces rapidly softens and it leads the sudden failure of RC beams. To prevent the shear failure, the JSCE standard specifications [1] have required a large amount of shear reinforcing bars. It causes the difficulty in filling concrete in construction sites. The use of fibers as shear reinforcement is one of the solutions for reducing the shear reinforcing bars in the structures without losing the shear strength. Many researchers [2, 3] have reported the effectiveness of fibers as shear reinforcement, focused exclusively on steel fibers.

The JSCE design guidelines for reinforced concrete piers with steel fibers [4] have regarded steel fibers as the reinforcement of concrete structures. The increment of shear strength by steel fibers has been expressed as a value κ, which was defined as a ratio of the shear carried by steel fibers to the shear carried by concrete and was equal to 1.0. Nevertheless, Watanabe et al. [3] concluded that all of the experimental values of κ (κ_{exp}) were more than 1.0. The post-cracking behavior of fiber reinforced concrete beams (FRC) was not considered in the design guidelines. The authors (Jongvivatsakul et al. [5]) proposed the evaluation method of shear carried by steel fibers by applying the fracture mechanics with shear behavior. The method was validated with the fiber reinforced concrete beams with steel fibers having length of 30 mm.

Recently, synthetic fibers have become more attractive than before due to its effectiveness for improving shear strength [2] and relatively inexpensive comparing with steel fibers. However, the influence of synthetic fibers and fiber length on shear carrying mechanism of FRC beams has not been deeply investigated and understood.

The objective of this paper is to investigate the shear carried by both steel and synthetic fibers. The shear resisting mechanism of four FRC beams with various kinds of fibers (i.e. material type and length) is examined. The evaluation method of shear carried by fibers using tension softening curves [5] is verified in order to confirm its applicability for investigating the shear capacity of FRC beams with various fibers.

2. EXPERIMENTAL PROGRAM

2.1 Materials

(1) Concrete

The materials used in this study were high-early strength portland cement, sand, coarse aggregates, and high-performance air-entraining water-reducing agent. Table 1 shows the mix proportion of concrete.

(2) Fibers

Four types of fibers were incorporated into concrete including steel fibers with length of 30 mm (SF30) and 60 mm (SF60), polypropylene fibers (PP) and polyvinyl alcohol fibers (PVA). Properties of fibers used in this study are summarized in Table 2. The surface of SF30, SF60 and PVA fibers was completely smooth, while the surface of PP fiber was rough. The intersection of two diagonal lines was observed on the surface of PP fiber. The volume fraction of fibers was identical as 1.0% of full volume of concrete in all specimens.

(3) Reinforcing materials

The longitudinal reinforcing bars were deformed steel with 25.4 mm of the nominal diameter and yield strength of 1006 N/mm^2. The stirrups with deformed steel of 6 mm in the nominal diameter were arranged as

*1 Ph. D. Candidate, Graduate School of Science and Engineering, Tokyo Institute of Technology, JCI Member
*2 Assistant Prof., Dept. of Civil Engineering, Tokyo Institute of Technology, Dr. E., JCI Member
*3 Assistant Senior Researcher, Concrete Structures, Railway Technical Research Institute, Ph. D., JCI Member
*4 Prof., Dept. of Civil Engineering, Tokyo Institute of Technology, Dr. E., JCI Member

Table 1 Mix proportion of concrete

G_{max} (mm)	W/C	Unit weight (kg/m^3)				
		W	C	S	G	SP
20	0.35	165	471	917	790	5.2

G_{max} = maximum size of coarse aggregate,
W = water, C = cement, S = fine aggregate,
G = coarse aggregate, SP = high-performance air-entraining (AE) water-reducing agent

Table 2 Properties of fibers

Name	L (mm)	ϕ (mm)	Density (kg/m^3)	Tensile strength (MPa)	E (GPa)	Shape of the end
SF30	30	0.62	7850	1050	210	Hooked
SF60	60	0.90	7850	1050	210	Hooked
PP	30	1.6×0.6	910	470	15	Straight
PVA	30	0.66	1300	960	23	Straight

L = Length, ϕ = Diameter, E = Elastic modulus

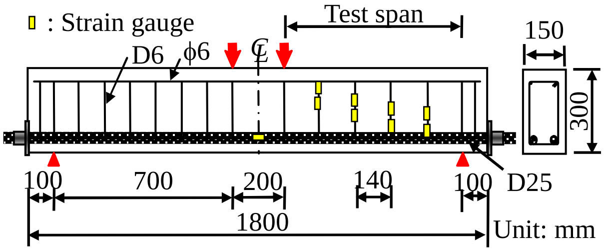

Fig. 1 Detail of a FRC beam

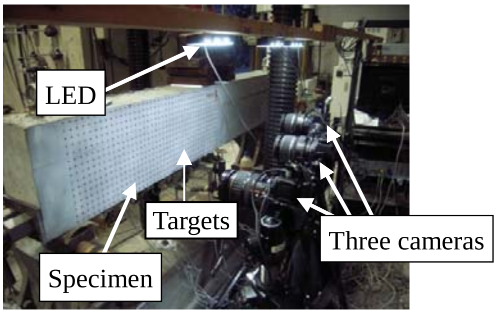

Fig. 2 Preparation of loading test

the shear reinforcement. The yield strength was 315 N/mm^2. Two round bars with the diameter of 6 mm were used as compression bars with the yield strength of 304 N/mm^2.

2.2 Test Specimens

Fig. 1 shows the dimension and reinforcing bars arrangement of a FRC beam. The specimens were rectangular FRC beams. The shear span (a) was 700 mm and effective depth (d) was 250 mm. The shear span to effective depth ratio (a/d) was 2.8. The longitudinal reinforcement ratio (p_w) was 2.7%. All specimens were controlled to fail in the right shear span by providing the less number of stirrups in the right shear span as shown in Fig. 1. Stirrups ratio in the test span (r_w) was 0.30% in all specimens. Four FRC beams were prepared, varying the type of fibers. The specimens were named according to the type of fibers used in the beams.

2.3 Loading Methods

Specimens were subjected to a four-point bending with simply-supported condition as illustrated in Fig. 1. Steel plates with 50 mm width were placed on the pin-hinge supports. Teflon sheets and grease were inserted between a specimen and supports in order to prevent the horizontal friction. At loading points, the steel plate with 65 mm width and 150 mm length were also placed. Fig. 1 shows the detailed loading arrangement along with the locations of loading points and strain gauges.

2.4 Measurements

Measuring items were the applied load, displacements of mid span and supporting points using four transducers, and strain of longitudinal steel bars and stirrups. The strain of longitudinal steel bars was measured at mid span by strain gauges while the strains of stirrups were measured at the locations that diagonal crack was expected to occur as shown in Fig. 1.

In addition, the crack surface displacement (u), which is the total displacement of crack on the direction of principal tensile strain, was measured from the image analyzing system developed by Higashi et al. [6]. A picture of loading test is shown in Fig. 2. In order to perform the image analysis, red targets with diameter of 5 mm were attached on the specimen surface with an interval of 20 mm. The image analyzing system can investigate the coordinate of these targets throughout the test span. As a result, the crack surface displacement can be calculated. During the loading test, photos of the specimen were taken by every 5 kN of the shear force using three digital cameras fixed on tripods. However, since the diagonal crack was expected to open rapidly near the peak load, some pictures were taken near the peak load with short time interval in order to capture the behavior at the peak exactly.

Besides, the length and angle of diagonal crack were measured from the visible diagonal crack at the peak load by using the software system, which supports analytical functions from image measurement to statistical data processing. The calibration process was conducted to define the length of one pixel in the image for the purpose that the measurement data in a pixel can be converted to the actual lengths. The images taken for measuring the crack surface displacements were also used to measure the crack length and angle of diagonal crack at the peak.

3. CALCULATION OF SHEAR FORCES AND EVALUATION OF SHEAR CARRIED BY FIBERS

3.1 Calculation of Shear Forces in FRC Beams

Considering the force acting at the diagonal crack in a FRC beam subjected to point loads (Fig. 3), it can be seen that the shear force is resisted by the shear carried by concrete (V_c), the shear carried by stirrups (V_s) and the shear carried by fibers (V_f). Consequently, the shear capacity (V) of fiber reinforced concrete beams is simplified as:

$$V = V_c + V_s + V_f \qquad (1)$$

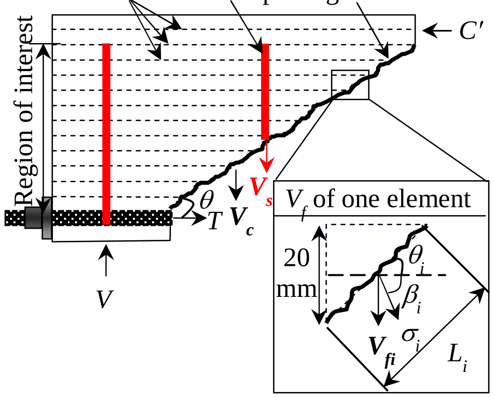

Fig. 3 Free body diagram of a FRC beam

Table 3 Properties and expression of tension softening curves

Type	f_c' (N/mm^2)	f_t (N/mm^2)	G_F (N/mm)	Expression
SF30	56.6	4.1	3.26	$\sigma = \begin{cases} 7.0 - 40.2u & \text{for } u < 0.13\text{ mm} \\ 1.85 - 0.55u & \text{for } u \geq 0.13\text{ mm} \end{cases}$
SF60	55.9	3.4	7.32	$\sigma = \begin{cases} 4.3 - 50.5u & \text{for } u < 0.04\text{ mm} \\ 2.3 - 0.31u & \text{for } u \geq 0.04\text{ mm} \end{cases}$
PP	58.8	3.9	3.02	$\sigma = \begin{cases} 3.9 - 23.5u & \text{for } u < 0.12\text{ mm} \\ 1.1 - 0.18u & \text{for } u \geq 0.12\text{ mm} \end{cases}$
PVA	59.9	3.6	1.79	$\sigma = \begin{cases} 3.6 - 18.2u & \text{for } u < 0.16\text{ mm} \\ 0.7 - 0.09u & \text{for } u \geq 0.16\text{ mm} \end{cases}$

f_c': compressive strength, f_t: tensile strength, G_F: fracture energy

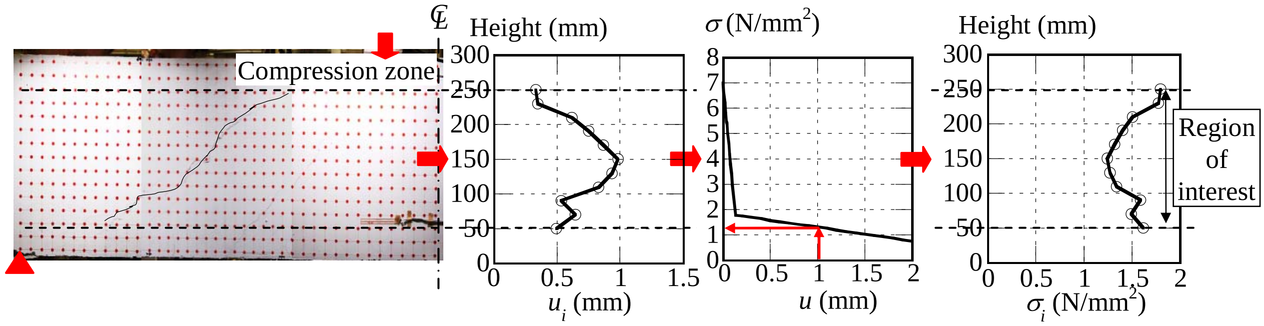

(a) Picture of a FRC beam at peak load (SF30) (b) u_i distribution (c) Tension softening curve (d) Stress distribution

Fig. 4 Investigation of tensile stress transferred across the diagonal crack

The shear carried by concrete (V_c) was calculated from Eq. 2 following the JSCE design guidelines [4]. Shear carried by stirrups (V_s) was obtained from Eq. 3. Hence, the experimental value of shear carried by fibers (V_{fexp}) can be obtained from Eq. 4.

$$V_c = 0.2 \cdot \sqrt[3]{f_c'} \cdot \sqrt[4]{1000/d} \cdot \sqrt[3]{100 p_w} \cdot b_w \cdot d \tag{2}$$

$$V_s = A_w f_{wy} (z\cot\theta / s) \tag{3}$$

$$V_{fexp} = V_{exp} - V_c - V_s \tag{4}$$

where, f_c' is the compressive strength of concrete (N/mm^2), d is the effective depth (mm), p_w is the longitudinal reinforcement ratio, b_w is the web thickness (mm), A_w is the cross section area of stirrups (mm^2), f_{wy} is the yield strength of stirrups (N/mm^2), z is the distance from location of compressive stress resultant to centroid of tension steel (z=7/8d) (mm), θ is the angle between the diagonal crack and horizontal line (degree) (see in Fig. 3), s is the stirrups spacing (mm), and V_{exp} is the experimental value of shear capacity (kN).

Furthermore, according to the JSCE design guidelines [4], the shear capacity of FRC members can be predicted by using Eq. 5. Thus, the experimental value of κ (= κ_{exp}) can be calculated by Eq. 6. However, it is noted that Eq. 5 was proposed for steel fiber reinforced concrete members.

$$V_{cal} = (1 + \kappa) \cdot V_c + V_s \tag{5}$$

$$\kappa_{exp} = V_{fexp} / V_c \tag{6}$$

where, V_{cal} is the predicted shear capacity (kN) and κ is the coefficient representing the effect of fibers (κ=1.0) [4].

3.2 Evaluation Method of Shear Carried by Fibers

The authors [5] have proposed the evaluation method of shear carried by steel fibers using tension softening curves. Tensile stress transferred across the diagonal crack (σ) can be converted from the crack surface displacement (u) using relationship between tensile stress and crack opening displacement of tension softening curves as shown in Fig. 4. In order to evaluate the shear carried by fibers precisely, the specimens were divided into 15 elements with a height of 20 mm (Fig. 3) corresponding to the interval of red targets in the image analysis. Crack surface displacement (u_i), length (L_i), angle of principal tensile strain (β_i), and angle of a diagonal crack (θ_i) of each element were investigated. By considering the force acting at a diagonal crack in a FRC beam due to the effect of fibers (Fig. 3), the force resisted by fibers was equal to the stress σ multiplied by the area of crack surface normal to direction of σ. The stress and shear forces were calculated for element by element. The force along the diagonal crack was obtained from the portion below the compression zone to the tip of

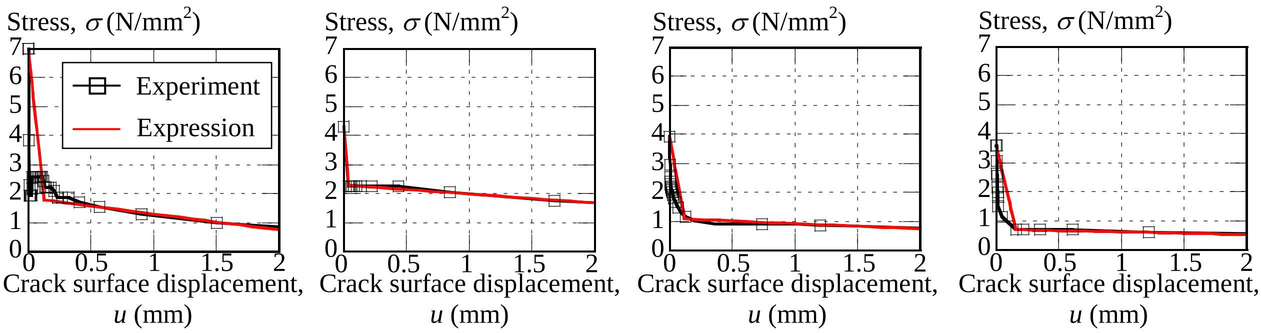

(a) SF30 (b) SF60 (c) PP (d) PVA

Fig. 5 Tension softening curves

Table 4 Summary of the calculation and experimental results

Specimen	Concrete properties		Information of diagonal crack				Calculation and experimental results						
	f_c' (N/mm^2)	f_t (N/mm^2)	u_{avg} (mm)	L (mm)	β_{avg} (°)	θ (°)	V_{exp} (kN)	V_c (kN)	V_s (kN)	V_{fexp} (kN)	κ_{exp}	V_{fcal} (kN)	V_{fexp}/V_{fcal}
SF30	55.3	3.05	0.67	387.3	63.3	36.8	158.8	56.3	41.6	60.8	1.08	72.6	0.84
SF60	61.9	3.69	1.08	378.3	64.6	38.2	196.3	58.4	39.6	98.3	1.68	96.2	1.02
PP	57.0	3.14	0.94	428.1	69.2	27.5	170.8	56.9	59.8	54.1	0.95	53.6	1.01
PVA	65.4	3.02	0.69	490.6	63.7	27.0	166.8	59.5	61.1	46.1	0.78	40.4	1.14

f_c': compressive strength, f_t: tensile strength, u_{avg}: average crack surface displacement at the peak, L: total crack length at the peak, β_{avg}: average angle of principal tensile strain at the peak, θ: angle between the diagonal crack and horizontal line.

diagonal crack in the tension zone and this zone was called the region of interest as seen in Fig. 3. The compression zone was the height of specimens from the top surface to the location of neutral axis at the peak, which was calculated from the displacements of targets obtained through the image analysis. The tip of diagonal crack stopped at the location of tensile bars. The summation of forces in region of interest was the shear carried by fibers. Consequently, the shear carried by fibers (V_{fcal}) can be expressed as follows [5]:

$$V_{fcal} = \sum_{i=1}^{n} \left(\sigma_i \cdot b_w \cdot L_i \cdot \cos(\beta_i + \theta_i - 90) \cdot \sin\beta_i \right) \qquad (7)$$

where, n is number of elements in the region of interest (n=11), σ_i is the tensile stress of element i (N/mm^2), L_i is the length of diagonal crack of element i (mm), β_i is the angle of principal tensile strain of element i (degree), and θ_i is the angle of diagonal crack of element i (degree).

This method [5] was validated for evaluation of shear carried by steel fibers having length of 30 mm with high accuracy. However, it has not been extended to fiber reinforced concrete beams with various types of fibers yet.

4. TENSION SOFTENING CURVES

The tension softening curves were obtained from the bending tests of notched beams conducted according to the standard of JCI [7]. The tension softening curves of four types of fiber reinforced concrete are shown in Fig. 5. Table 3 lists the compressive strength and fracture energy of concrete of those notched beams. By using a least-square data-fitting procedure based on solution of an inverse, the shape of bilinear curves of tension softening diagram can be obtained as shown in Table 3. As seen in Fig. 5, the tension softening behavior was different depending on type of fibers. SF60 can resist the highest stress in post-peak region. Steel fibers (SF30 and SF60) can transfer higher stress than synthetic fibers (PP and PVA). Two kinds of fibers' failure were observed in the notched beam tests. SF30 and SF60 were failed in pulled-out mechanism while PP and PVA showed both pulled-out and cut-off mechanism. It was because steel fibers had higher tensile strength than PP and PVA.

5. EXPERIMENTAL RESULTS

5.1 Effect of Fibers on Shear Behavior

Table 4 summarizes the concrete properties, information of diagonal crack, calculated shear forces and shear forces obtained from the loading tests of FRC beams. The shear capacity (V_{exp}) of SF60 was the highest among four specimens. The difference of V_c between each specimen was slight since the compressive strength of concrete was not significantly varied. Whereas V_s was certainly different in each specimen due to the deviation of θ that was measured as the angle between the diagonal crack and the horizontal line (Fig. 3). The values of θ are presented in Table 4. SF60 provided the largest θ among all specimens. Fig. 6 shows average strain of stirrups in the test span. It was observed that stirrups in the test span were yielded before the ultimate load. Synthetic fibers (PP and PVA) led the early yielding of stirrups before SF30 and SF60 due to the lower materials' modulus of elasticity. Considering the shear carried by fibers, it was found that V_{fexp} of SF60 was the largest

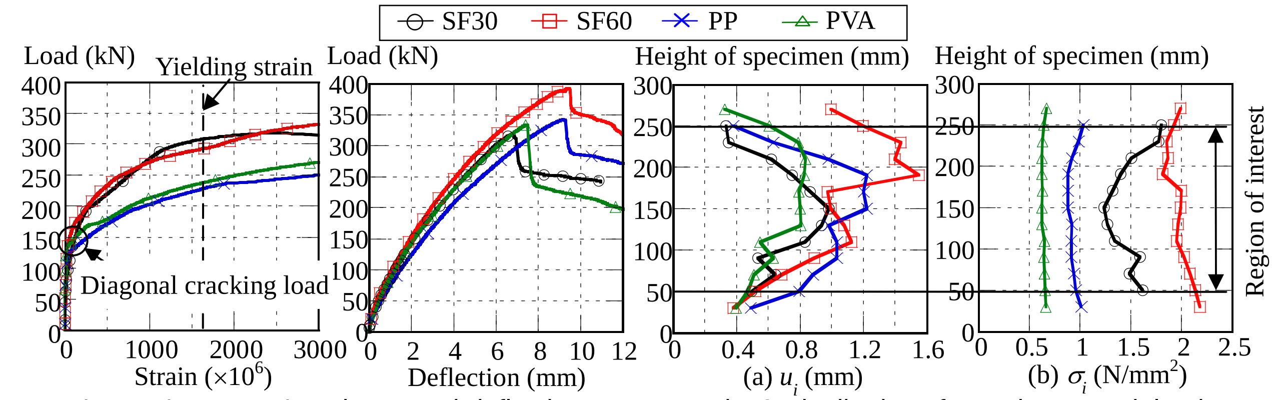

Fig. 6 Stirrups strain Fig. 7 Load-deflection curves Fig. 8 Distribution of u_i and σ_i at peak load

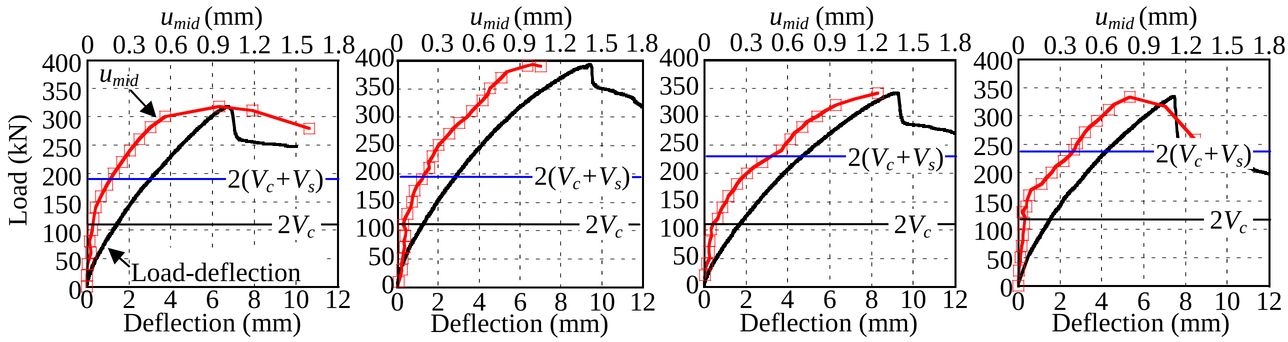

(a) SF30 (b) SF60 (c) PP (d) PVA

Fig. 9 Development of crack surface displacement and deflection

resulting in the largest shear capacity. The value of κ_{exp} of SF30 and SF60 was more than 1.0. On the other hand, κ_{exp} of PP and PVA was less than 1.0. Steel fibers can enhance V_{fexp} more effectively than synthetic fibers. The difference of type of fibers caused the difference of V_{exp}, V_{fexp} and also the load level that stirrups were yielded.

5.2 Load-Deflection Curves

The relationship between the applied load and the mid span deflection are presented in Fig. 7. The load-deflection response was linear prior to cracking. After the initiation of first flexural cracking, the load-deflection response changed to non-linear behavior. Later, the diagonal crack was observed in the test span and propagated to loading point and support. In the pre-peak region, the propagation of diagonal crack stopped and the slope of load-deflection curve became flat. Then the diagonal tension failure occurred and concrete in compression zone was crushed. The same behavior of load-deflection response can be observed in all specimens.

5.3 Diagonal Cracking Behavior

The diagonal cracking data, which were u_i, L_i, β_i, and θ_i, of each element were investigated based on the pictures taken at the peak load.

(1) Crack surface displacement (u_i)

Fig. 8(a) presents the value of u_i along the height of diagonal crack at the peak load. The diagonal crack surface displacement was larger at around the middle height of specimens compared with the u_i at the top and the bottom of specimens because there was compression zone at top of specimens and restraint by longitudinal reinforcing bars at the bottom part of specimens. The region of interest was considered from 50-250 mm in all specimens correspondingly in this paper. Nevertheless, the influences of types of fibers and stirrup ratio on the location of region of interest have not been clearly understood yet. Therefore, a number of FRC beams with various types of fibers will be tested in the future in order to clarify the location of region of interest. Table 4 presents the average value of crack surface displacement (u_{avg}) of the diagonal crack in the region of interest shown in Fig. 8. The result showed that u_{avg} of SF60 was the widest because u_i around top surface showed larger value than the other specimens. It is because SF60 had longer length than other fibers and also effect of anchorage (hooked end).

Fig. 9 shows the crack surface displacements measured at the middle height of the specimens (u_{mid}), where was 150 mm, in the top horizontal axis together with the load-deflection curve. It can be seen that u_{mid} of specimens with both steel fibers and synthetic fibers increased drastically before the peak load.

(2) Diagonal crack length (L)

The crack length (L) is the length of a diagonal crack in the region of interest. PP and PVA provided longer diagonal crack length than specimens with steel fibers (SF30 and SF60) as shown in Table 4 because the diagonal cracks near the longitudinal steel bars had low inclination.

(3) Angles of principal tensile strain (β_i) and diagonal crack (θ)

Table 4 presents the average value of β_i in the region of interest. β_{avg} did not change significantly among these specimens. On the other hand, by considering θ, it was found that SF30 and SF60 revealed the steepest diagonal crack than the other specimens. Steel fibers provided the steeper diagonal crack than synthetic fibers.

5.4 Calculated Shear Carried by Fibers

The tensile stress transferred across the diagonal crack at the peak load was investigated from crack surface displacement and relationship of tension softening curves listed in Table 3 as mentioned in Section 3.2. Fig. 8(b) shows the stresses across the diagonal crack in FRC beams at the peak load. The larger stress could be resisted at top and bottom parts of specimens due to the smaller u_i. SF60 can resist the highest stress resulting in the largest V_{fexp} whereas PP and PVA resisted relatively lower stress across the diagonal crack. The stress distribution of PVA was not varied because the slope of tension softening curve of PVA was almost flat when $u \geq 0.16$ mm.

The shear carried by fibers (V_{fcal}) was calculated by Eq. 7 and summarized in Table 4. Fig. 10 presents the comparison of the experimental results and calculated values. The mean value of the experimental value to calculated value of the shear carried by fibers was 1.00 with the coefficient of variation (*C.V.*) of 12.5%. Therefore, it can be implied that the proposed method can evaluate the shear carried by fibers of FRC beams. This method can be used even the material types and length of fibers were varied since the tension softening curve can reflect the characteristic of each fiber. The applicability of tension softening curves to examine the stress transferred across the diagonal crack of FRC beams was proved. However, due to the limitation of number of specimens in the present study, a number of specimens with various types of fibers should be tested in the future in order to validate the applicability of the proposed method.

6. CONCLUSIONS

(1) Shear capacity of FRC beams with 60-mm steel fibers was the largest comparing with 30-mm steel fibers, polypropylene and polyvinyl alcohol because 60-mm steel fibers revealed the highest shear contribution by fibers.

(2) The value of κ_{exp} was more than 1.0 in case of steel fibers. On the other hand, κ_{exp} of polypropylene and polyvinyl alcohol was less than 1.0. Steel fibers were more effective as shear reinforcement than synthetic fibers.

(3) The specimen with 60-mm steel fibers provided the widest crack surface displacement at the peak load because of the effects of fiber length and anchorage. However, it was most effective to transfer stress across the crack due to the good post peak region of its tension softening curve.

(4) The intensity of stress transferred across the diagonal crack of FRC beams at the peak load can be ranked from the highest intensity as the beam with 60-mm steel fibers, 30-mm steel fibers, polypropylene and polyvinyl alcohol, respectively. In FRC beams, steel fibers can transfer more stress across the diagonal crack than synthetic fibers resulting in the higher shear transferred force by fibers.

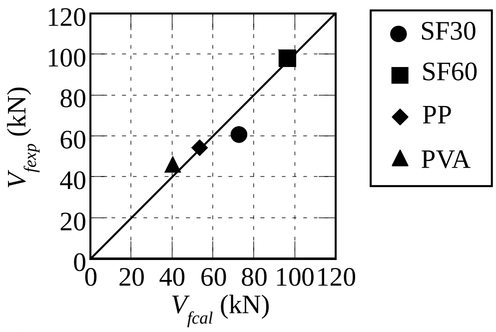

Fig. 10 Comparison of V_{fexp} and V_{fcal}

(5) The evaluation method of shear contribution of fibers was presented. The calculated shear carried by fibers showed good agreement with experimental results even various material types and length of fibers.

ACKNOWLEDGEMENT

The authors acknowledge the support from the Center for Urban Earthquake Engineering (CUEE).

REFERENCES

[1] JSCE, "Standard Specifications for Concrete Structures-2002, Structural Performance Verification", JSCE Guidelines for Concrete, No. 3, 2005, pp. 76-83.

[2] Li, V. C., Ward, R., and Hamaza, A. M., "Steel and Synthetic Fibers as Shear Reinforcement", ACI Materials Journal, Vol. 89, No. 5, Sept.-Oct. 1992, pp. 499-508.

[3] Watanabe, K., Kimura, T., Kodama, T., Kita, S., Odera, I., and Niwa, J., "Shear Reinforcement for RC Linear Members by a Combination of Steel Fibers and Shear Reinforcing Bars", Journal of Materials, Concrete Structures and Pavements, JSCE, Vol. 65, Jul. 2009, pp. 322-331. (in Japanese)

[4] JSCE, "Guidelines of Design for RSF Piers", Concrete Library 97, 1999, p. 15. (in Japanese)

[5] Jongvivatsakul, P., Watanabe, K., Matsumoto, K., and Niwa, J., "Evaluation of Shear Carried by Steel Fibers of Reinforced Concrete Beams Using Tension Softening Curves", Journal of Materials, Concrete Structures and Pavements, JSCE, Vol. 67, No. 4, Oct. 2011, pp. 493-507.

[6] Higashi, H., Watanabe, K., and Niwa, J., "Image Analysis for Failure Mode of RC Beams with Fractured Longitudinal Reinforcement", Proceedings of the JCI, Vol. 31, No. 2, Jul. 2009, pp. 727-732. (in Japanese)

[7] JCI, "Method of Test for Fracture Energy of Concrete by Use of Notched Beams", Japan Concrete Institute Standard, 2003.